

# A cellulose-based bioassay for the colorimetric detection of pathogen DNA

Deepika Saikrishnan · Madhu Goyal · Sharon Rossiter · Andreas Kukol

Received: 28 July 2014 / Revised: 1 October 2014 / Accepted: 8 October 2014 / Published online: 30 October 2014  
© Springer-Verlag Berlin Heidelberg 2014

**Abstract** Cellulose-paper-based colorimetric bioassays may be used at the point of sampling without sophisticated equipment. This study reports the development of a colorimetric bioassay based on cellulose that can detect pathogen DNA. The detection was based on covalently attached single-stranded DNA probes and visual analysis. A cellulose surface functionalized with tosyl groups was prepared by the *N,N*-dimethylacetamide–lithium chloride method. Tosylation of cellulose was confirmed by scanning electron microscopy, Fourier transform infrared spectroscopy and elemental analysis. Sulfhydryl-modified oligonucleotide probes complementary to a segment of the DNA sequence IS6110 of *Mycobacterium tuberculosis* were covalently immobilized on the tosylated cellulose. On hybridization of biotin-labelled DNA oligonucleotides with these probes, a colorimetric signal was obtained with streptavidin-conjugated horseradish peroxidase catalysing the oxidation of tetramethylbenzidine by H<sub>2</sub>O<sub>2</sub>. The colour intensity was significantly reduced when the bioassay was subjected to DNA oligonucleotide of randomized base composition. Initial experiments have shown a sensitivity of 0.1 μM. A high probe immobilization efficiency (more than 90 %) was observed with a detection limit of 0.1 μM, corresponding to an absolute amount of 10 pmol. The detection of *M. tuberculosis* DNA was demonstrated using this technique coupled with PCR for biotinylation of the DNA. This work shows the potential use of tosylated cellulose as the basis for point-of-sampling bioassays.

**Keywords** Cellulose tosylation · Oligonucleotide probe · Visual detection · *Mycobacterium tuberculosis*

D. Saikrishnan · M. Goyal · S. Rossiter · A. Kukol (✉)  
School of Life and Medical Sciences, University of Hertfordshire,  
Hatfield AL10 9AB, UK  
e-mail: a.kukol@herts.ac.uk

## Introduction

Biosensors and bioassays play an important role in clinical diagnosis, food processing safety applications, environmental monitoring and forensic science [1]. Biosensor technology growth in the last couple of decades was primarily due to the development of various advanced biorecognition, transduction and signal processing elements. The biorecognition elements used in biosensors are enzymes [2, 3], ion channels [4], antibodies [5, 6], microorganisms [7] and nucleic acids such as deoxyribonucleic acid (DNA) [8], peptide nucleic acid [9], ribonucleic acid (RNA) [10], microRNA and locked nucleic acids [11]. The use of single-stranded DNA has increased owing to its stability, sensitivity and high specificity arising from the ability of complementary strands to form a duplex as well as owing to the commercial availability of custom oligonucleotides with chemical modifications. Various transduction methods have been applied—for example, electrochemical [12, 13] and optical methods [14]—leading to numerous kinds of signal processing. In electrochemical transduction of DNA hybridization, detection is based on electrical current signal changes of redox molecule labels or on changes in parameters of the biomolecular layer, such as capacitance and conductivity [11]. Most electrochemical DNA biosensors make use of differential pulse voltammetry, cyclic voltammetry, impedance, amperometric, potentiometric, surface plasmon resonance and piezoelectricity techniques [15–17]. A differential-pulse voltammetry based DNA biosensor to detect Enterobacteriaceae DNA including a target DNA recycling system with a sensitivity of 8.7 fM was recently developed [18]. Impedimetric sensors constructed with gold nanoparticles and graphene oxide modifications to a carbon electrode have been reported as high-sensitivity DNA biosensors with detection limits around 11 fM [19]. An anodic aluminium oxide microfluidic 3D channel was used as an electrode for DNA probe immobilization and target

detection using cyclic voltammetry to measure electrochemical response using redox indicators,  $[\text{Fe}(\text{CN})_6]^{4+}$  and/or  $[\text{Ru}(\text{NH}_3)_6]^{3+}$  [20]. Although electrochemical biosensors are widely used in biosensing, providing high sensitivity, these sensors are commonly associated with non-specific binding leading to poor selectivity and also to fouling of electrodes, especially with real samples such as blood. In addition, the construction and manufacture of electrochemical sensors is not cost-effective and this makes them a less preferred choice for use in diagnostic sensors despite their advantages [15].

DNA hybridization can also be detected optically using fluorescence, surface plasmon resonance, chemiluminescence, colorimetry, interferometry or surface-enhanced Raman scattering spectroscopy (reviewed in [21]). Of all the optical methods, colorimetric assays are preferred for initial diagnostic tests as they give visual readouts and have good stability, and often reagents are less expensive, and thus these assays are suitable for low-resourced areas [22]. Enzyme labels such as horseradish peroxidase (HRP) [17, 23] and metal nanoparticles, especially gold nanoparticles, have been widely used for colorimetric nucleic acid assays in solution and on solid surfaces [24–26]. Although colorimetric tests are favourable, there is a compromise on sensitivity when compared with electrochemical biosensors. This disadvantage of colorimetric and optical sensors can be attributed to the high concentrations of sample required to produce significant optical or visual signals.

Various materials have been routinely used as a basic surface to construct biosensors, ranging from glass supports [27], polystyrene [28] and gold nanoparticles [29, 30] to cellulose in its various forms, including paper [31, 32]. Paper as a biosensing surface has many advantages over other materials—it is a very good filter and barrier medium, it is cost-effective, it can be easily coated or impregnated, it is biodegradable, it has high porosity, it is conducive to lateral flow and it has low non-specific absorption of biomolecules [33]. These properties of paper have led to its use in a number of microfluidic devices for many applications in diagnostics [8, 22, 30, 34–37]. Another important property that contributes to the wide use of cellulose for immobilization of biomolecules is the presence of hydroxyl groups, which can be subjected to many chemical reactions, such as oxidation [38], esterification [39], acylation and tosylation [40] among others [41], that allow chemical groups of a biomolecule to covalently bind to the cellulose. Although there has been a surge in the number of colorimetric biosensors that use paper microfluidics, there are few simple assays that address the issue of pathogen diagnostics in high-burden, low-resourced areas; most colorimetric biosensors are primarily targeted at food-borne bacteria [42–44]. In this work, we demonstrate the use of tosylated cellulose strips for the immobilization of sulfhydryl-modified oligonucleotide probes and visual detection of target DNA. The sequences correspond to the IS6110

transposable element present in *Mycobacterium tuberculosis* and colorimetric detection is performed with streptavidin-conjugated HRP and chromogenic tetramethylbenzidine substrate. The sensitivity and specificity of the system is evaluated with synthetic DNA and DNA isolated from the pathogen.

## Materials and methods

### Tosylation of cellulose

Tosylated cellulose was prepared by downscaling and modifying a method described by Rahn et al. [45]. First, 2.0 g microcrystalline cellulose (Avicel® PH-101, Sigma-Aldrich, UK) was heated in 40 mL of *N,N*-dimethylacetamide at 160 °C for 1 h with stirring. After the solution had been cooled to 100 °C, 4.0 g anhydrous lithium chloride was added, and then the reaction mixture was cooled further to room temperature. Then, 5 mL triethylamine was added to the highly viscous solution. This viscous solution was then cooled in an ice bath to 8–10 °C. Next, 4.0 g of *p*-toluenesulfonyl chloride dissolved in 6 mL *N,N*-dimethylacetamide was added to the solution. After 24 h, the reaction mixture was poured into glass petri dishes, immersed in ice-cold water and allowed to precipitate for 2 h. As a modification of the original method [45], the precipitated sheets were washed in ice-cold water and allowed to dry between sheets of strong tissue paper for 24 h. A control cellulose film was prepared with a similar procedure without addition of tosyl chloride. The tosylated and control cellulose strips were then subjected to attenuated total reflection Fourier transform infrared (FTIR) spectroscopy, scanning electron microscopy (SEM) and elemental analysis.

### FTIR analysis

A Nicolet 6700 FTIR instrument (Thermo Scientific, UK) with a diamond attenuated total reflection accessory was used to analyse the samples. The attenuated total reflection FTIR spectra of cellulose powder, control cellulose film and tosylated cellulose were recorded with 30 scans per spectrum and a resolution of 4  $\text{cm}^{-1}$  using a deuterated triglycine sulfate detector. The spectrum was processed with level 2 zero filling and Norton–Beer apodization.

### SEM analysis

Tosylated cellulose, control cellulose film, Whatman filter paper and cellulose powder were analysed with a JEOL JCM-7500 scanning electron microscope in the secondary electron image mode. All specimens were coated with a layer of gold approximately 30 nm thick.

Low accelerating voltages of 5 or 10 kV were used for the measurement. The measurements were made with spot sizes of 31 and 35 and at working distances (from the lens) of 15 and 28 mm.

#### Elemental analysis

Elemental analysis was performed by Medac (Chobham, UK) to find the percentage composition of sulfur and chlorine in the samples; this was used for determining the degree of substitution. The degree of substitution is defined as the number of tosylated hydroxyl groups per glucose unit and was calculated from the percentage of sulfur ( $S\%$ ) obtained from elemental analysis using the formula  $DS_S = (S\% \times M_G) / [(M_S \times 100) - (M_{Tos} \times S\%)]$  [45], where  $M_G$  is the molecular mass of a glucose unit ( $180.16 \text{ g mol}^{-1}$ ),  $M_S$  is the molecular mass of sulfur ( $32.06 \text{ g mol}^{-1}$ ) and  $M_{Tos}$  is the molecular mass of a tosyl group ( $155.19 \text{ g mol}^{-1}$ ).

#### Immobilization of oligonucleotide probes

All synthetic oligonucleotides were obtained from Eurogentec (Belgium). One hundred microlitres of a  $2.5 \mu\text{M}$  solution of the 5'-end hexanethiol (SH) and hexaethyleneglycol (HEG) spacer modified oligonucleotide (29 nt), 5'-SH-HEG-GGCG AACCTGCCAGGTCGACACATAGG-3' (IS6110 element of *M. tuberculosis*), containing dithiothreitol ( $300 \mu\text{M}$ ) and phosphate buffer solution (PBS;  $92 \text{ mM}$ , pH 7.2) was pipetted onto the tosylated cellulose surface placed in a closed petri dish and was allowed to react for 16–18 h in the dark at room temperature.

#### Synthetic target hybridization

5'-Biotinylated target (complementary to the probe) oligonucleotides, 5'-biotin-CCTATGTGTCGACCTGG GCAGGG TTCGCC-3' and a randomized (non-complementary) oligonucleotide of the same base composition, 5'-biotin-GTGTGCCCATCGTACGCGAGTCGTGCGT-3', were prepared to a final concentration of  $1 \mu\text{M}$  with hybridization buffer [ $270 \text{ mM NaCl}$ ,  $4.5 \text{ mM MgCl}_2 \cdot 6\text{H}_2\text{O}$  and  $22.5 \text{ mM tris}(\text{hydroxymethyl})\text{aminomethane}$  (Tris), pH 8.3], and  $100 \mu\text{L}$  of each solution was pipetted on individual tosylated cellulose strips with immobilized probes and incubated for 1 h at  $60^\circ \text{C}$ . After incubation, the samples were washed three times with sterile distilled water for 15, 5 and 5 min, respectively, to remove any unbound probe and target/random oligonucleotides. Then,  $100 \mu\text{L}$  of hybridization buffer was pipetted onto probe-immobilized tosylated cellulose strips, and these were used as negative controls. The experiment was performed in triplicate.

#### Detection

After hybridization, the cellulose strips were washed with freshly distilled water three times for 15, 5 and 5 min at room temperature. The strips were then blocked with 5 mL of 10 % blocking solution containing non-fat milk powder (ECL blocking agent, GE Healthcare) and 0.1 % PBS–Tween 20 for 1 h at room temperature. After the blocking step, the samples were washed in PBS–Tween 20 three times for 15, 5 and 5 min. Then,  $50 \mu\text{L}$  of streptavidin–HRP conjugate in 0.1 % PBS–Tween 20 (1:1,000) was added to each sample and the mixtures were incubated for 1 h and washed in PBS–Tween-20 three times for 15, 5 and 5 min. The HRP substrate 3,5,3',5'-tetramethylbenzidine at a concentration of  $0.55 \text{ mg mL}^{-1}$  was prepared with 1 mL dimethyl sulfoxide (DMSO),  $20 \mu\text{M H}_2\text{O}_2$  (30 % w/v) and buffer ( $4.5 \text{ mM CaCl}_2 \cdot 2\text{H}_2\text{O}$ ,  $22.5 \text{ mM citric acid}$ ,  $45 \text{ mM NaH}_2\text{PO}_4 \cdot \text{H}_2\text{O}$ ). Then,  $75 \mu\text{L}$  of this solution was added onto each cellulose sample and observed for a colour change. Once the colour had developed, the sample was scanned with a flatbed scanner and quantified with ImageJ [7].

#### Image analysis

ImageJ 1.47v [46] was used to measure the signal intensity from images of assay samples produced by a scanner. Each image was split into three channels—red, blue and green. The red channel image provided the highest contrast and was used for analysis. The image was inverted, so lighter grey areas (higher pixel intensities) corresponded to a detection signal. The mean pixel intensity of an area was measured using the oval tool to maintain a constant area measurement.

#### Quantification of probe immobilization

The amount of a fluorescent probe immobilized on cellulose was estimated by subtracting the cumulative amount of probe removed in successive washing steps from the total amount of probe added onto cellulose. 5'-SH-HEG-GGCGAACCTGGC CCAGGTCGACACATAGG-fluorescein-3' oligonucleotide probes (purified by reversed-phase high-performance liquid chromatography) were purchased (Eurogentec, Belgium). Oligonucleotide probe solutions ( $100 \mu\text{L}$ ) at concentrations between  $0.5$  and  $5 \mu\text{M}$  were prepared with dithiothreitol ( $300 \mu\text{M}$ ) and PBS ( $92 \text{ mM}$ , pH 7.2). The samples were diluted to 1 mL with PBS, and the initial fluorescence intensity was measured with a fluorimeter with an excitation wavelength of  $490 \text{ nm}$  and an emission wavelength of  $520 \text{ nm}$ . The solutions were pipetted onto individual tosylated strips and allowed to react for 18 h; the strips were then washed three times in 5 mL fresh PBS. Each set of washings was collected individually, and the fluorescence intensity was measured with a fluorimeter. The third wash did not yield any

fluorescence signal and hence further washing of the samples was not required. The difference between the integrated peak area of the solutions and the cumulative peak areas of the three washings were calculated to measure the amount of probe immobilized.

### Sensitivity

A series of solutions of target and random oligonucleotides of various concentrations (1, 0.5, 0.1, 0.05 and 0.01  $\mu\text{M}$ ) were prepared with hybridization buffer (270 mM NaCl, 4.5 mM  $\text{MgCl}_2 \cdot 6\text{H}_2\text{O}$  and 22.5 mM Tris, pH 8.3). Then, 100  $\mu\text{L}$  of each solution was pipetted onto the tosylated cellulose strips, and hybridization was performed for 1 h at 60  $^\circ\text{C}$ . Detection was performed using the method described earlier.

### Specificity

To analyse the specificity of the method, 1  $\mu\text{M}$  solutions of 5'-biotin-labelled target, single-base mismatch, double base mismatch, triple base mismatch and randomized oligonucleotide sequences with respect to the probe sequence were prepared with dithiothreitol (300  $\mu\text{M}$ ) and PBS (92 mM, pH 7.2). Then, 100  $\mu\text{L}$  of each solution was pipetted onto probe-immobilized tosylated cellulose strips. The strips were hybridized for 1 h at 60  $^\circ\text{C}$ , and detection was performed as described earlier.

### Hybridization time

Solutions (1  $\mu\text{M}$ ) of target and random oligonucleotide sequences were prepared with hybridization buffer (270 mM NaCl, 4.5 mM  $\text{MgCl}_2 \cdot 6\text{H}_2\text{O}$  and 22.5 mM Tris, pH 8.3). Then, 100  $\mu\text{L}$  of each solution was pipetted onto probe-immobilized tosylated cellulose strips, and hybridization was performed for 0.5, 1, 1.5 and 2 h at 60  $^\circ\text{C}$ . Detection was performed as before. This experiment was performed in duplicate.

### PCR

PCR was performed on H37Rv *M. tuberculosis* DNA (provided by Brian Robertson, Imperial College, London, UK) to amplify the specific regions and also to incorporate biotin labels in the sample. Primers were chosen from the IS6110 transposable element. Two sets of primers with biotin labels were obtained from Invitrogen. One set was used to amplify a region containing the complementary region with respect to the probe. The primers for complementary sequence amplification were from *M. tuberculosis* transposable insertion element IS6110 at position 791 (forward primer; 5'-TAACCGGCTGTGGTAGCA-3') and at position 864 (reverse primer; 5'-CGGTGACAAAGGCCACGTA-3') and the other set was used to amplify the region non-specific to the probe, also from

IS6110 at position 1062 (forward primer; 5'-CCGAGGCAGGCATCCA-3') and at position 1132 (reverse primer; 5'-GATCGTCTCGGCTAGTGCATT-3'). The PCR was performed in a 50- $\mu\text{L}$  volume containing *Taq* polymerase (1 U  $\mu\text{L}^{-1}$ ), forward and reverse primers (25.6 nM), 1 $\times$  reaction buffer,  $\text{MgCl}_2$  (3 mM), dNTPs (1  $\mu\text{M}$ ), template DNA (7.2 ng  $\mu\text{L}^{-1}$ ) and sterile distilled water. The amplification parameters were as follows: 94  $^\circ\text{C}$  for 5 min followed by 40 cycles at 94  $^\circ\text{C}$  for 1 min, 58  $^\circ\text{C}$  (complementary region) and 60  $^\circ\text{C}$  (non-complementary region) for 1 min, and 72  $^\circ\text{C}$  for 1 min. After the 40 cycles, the samples were heated at 72  $^\circ\text{C}$  for 10 min. The samples were then subjected to gel electrophoresis in 2 % agarose gel.

### Assay with PCR product

The PCR products were used without further purification. The products obtained were heated to 95  $^\circ\text{C}$  to denature the helical duplex and then rapidly cooled in ice. Then, 10  $\mu\text{L}$  of the PCR product was added to 90  $\mu\text{L}$  hybridization buffer and the mixture was added onto probe-immobilized tosylated strips and hybridization was performed at 59  $^\circ\text{C}$  for 1 h. The samples were washed three times with fresh distilled water for 15, 5 and 5 min, respectively. PCR controls without template DNA were used as controls for the assay. The experiment was conducted in triplicate. The detection was performed as mentioned earlier.

## Results and discussion

### Tosylation of cellulose

Cellulose was tosylated successfully with modifications to the method described by Rahn et al. [45]. The infrared absorption spectrum of tosylated cellulose in Fig. 1 (spectrum a) shows characteristic peaks at 814  $\text{cm}^{-1}$  (aromatic C-H bend vibration), 1,177  $\text{cm}^{-1}$  (symmetric  $\text{SO}_2$  stretch vibration), 1,364  $\text{cm}^{-1}$  and 1,598  $\text{cm}^{-1}$  (aromatic C-C bend vibrations), which are not present in the spectra of control cellulose films and cellulose powder (Fig. 1, spectra b and c). These results show that cellulose was successfully tosylated and that the modifications that were made to the reported tosylation method did not impact the formation of the tosylated cellulose product. The SEM images show the difference in the structural appearance of the tosylated cellulose, control cellulose film, Whatman filter paper and cellulose powder (Fig. 2). The SEM image of tosylated cellulose in Fig. 2a had a very porous and uneven surface. In contrast, in Fig. 2b, the control cellulose film had a smooth surface with bigger lumps of material appearing at random locations, possibly caused by undissolved lithium chloride. Tosyl chloride disrupts the formation of



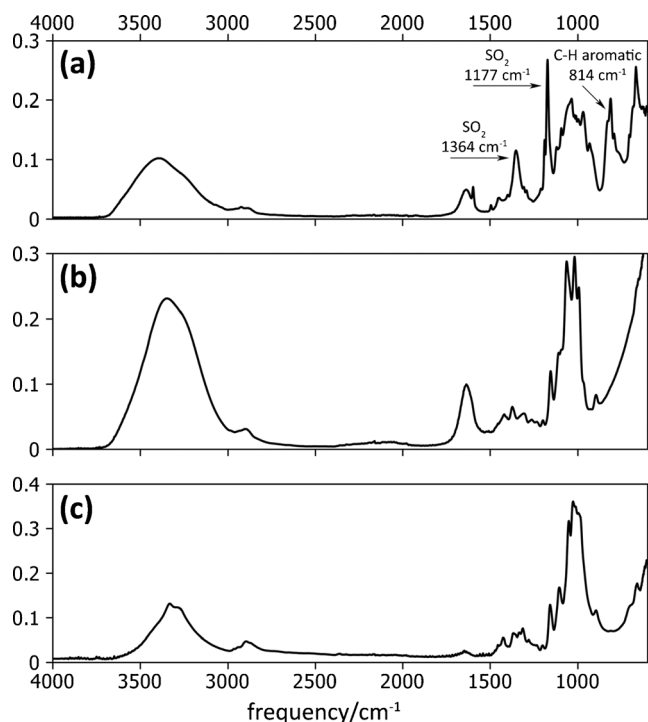


**Fig. 1** Fourier transform infrared spectra of tosylated cellulose (a), cellulose film (b) and cellulose powder (c)

dimethylacetamide  $\text{Li}^+$  and forms the tosyl derivative of cellulose, which does not occur in the control cellulose film, and this may be the reason for the difference in the surface appearance. The SEM images in Fig. 2c and d show that Whatman filter paper consists of a network of fibres, whereas

cellulose powder has an uneven surface with thicker lumps of material.

Elemental analysis of tosylated cellulose and control cellulose films was performed. The elemental analysis showed the expected high sulfur content relative to the chlorine content. However, the chlorine content is higher than reported previously [45]. This may be a consequence of not subjecting the sample to washing in ethanol and re-precipitation in acetone. This step was avoided to retain the samples as rigid materials to create a paper-like surface for biomolecule immobilization. The degrees of substitution of hydroxyl groups with sulfur ( $\text{DS}_\text{S}$ ) in tosylated cellulose are shown with the elemental analysis results in Table 1. The absolute maximum value for  $\text{DS}_\text{S}$  obtainable for tosylated cellulose is 3.0, since there are three hydroxyl groups per glucose unit. The  $\text{DS}_\text{S}$  of 0.28 (9.6 %) and 0.3 (10 %) are much smaller than the value of 1.36 (45.6 %) obtained previously for a similar cellulose starting material [45]. The degree of substitution has a direct impact on the sensitivity of the system because it determines the number of sites available for biomolecule immobilization. However, as demonstrated in this work, this material can be used for biosensing applications.

#### Quantification of probe immobilization

To estimate the amount of probe oligonucleotides that were immobilized covalently on the tosylated cellulose surface, fluorescein-labelled oligonucleotides at various concentrations were used for immobilization. The amount of probe covalently bound to tosylated cellulose was calculated indirectly by determining the amount of probe that did not bind to

**Fig. 2** Scanning electron microscope images of **a** tosylated cellulose, **b** cellulose film, **c** Whatman grade 40 filter paper and **d** cellulose powder

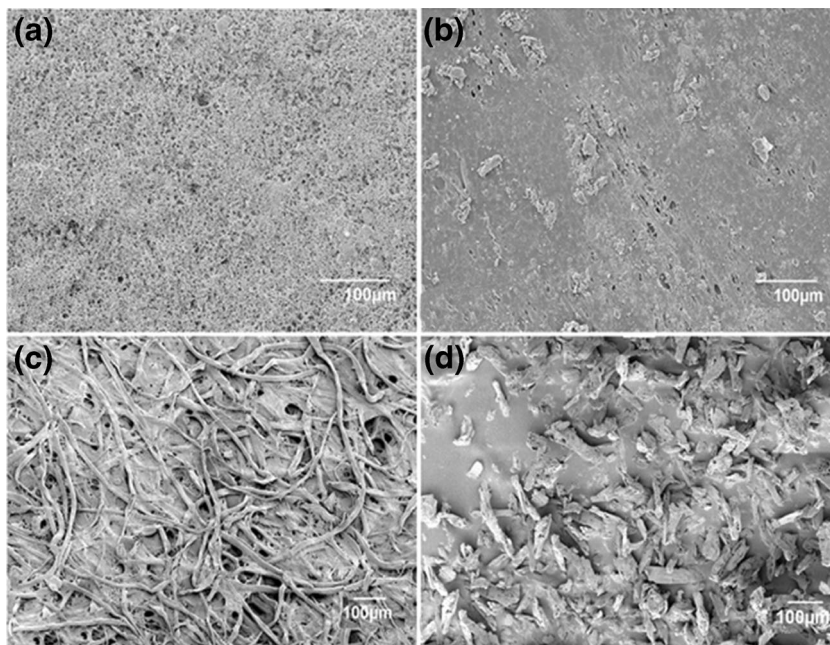


**Table 1** Elemental analysis of control films and tosylated cellulose and the degree of substitution in these samples calculated on the basis of the sulfur content

Substance	Elemental analysis		Degree of substitution of sulfur (no. of units)
	Sulfur (%)	Chlorine (%)	
Cellulose (control)	<0.10	2.70	0.0066
Replicate	<0.10	2.68	0.0066
Tosylated cellulose	4.05	2.72	0.283
Replicate	4.33	2.84	0.308

cellulose, but could be washed off. The results show that there was an increase in covalent attachment with increasing amount of probes added (Fig. 3). The linear increase is observed only until 0.25 nmol, after which there was a fluctuating amount of covalent attachment of the probe. We suggest that when more than 0.25 nmol probe is added to the modified cellulose surface, this leads to non-specific adsorption of the probe, including entrapment in the cellulose fibre network. The fluctuations in the amount of probe immobilization is then caused by variation in the cellulose sample. Producing tosylated cellulose paper in an automated paper manufacturing process would eliminate these fluctuations. For the present study, to ensure a reproducible quantity of probe for immobilization, we used a final quantity of 0.25 nmol, corresponding to a concentration of 2.5  $\mu\text{M}$  in 100  $\mu\text{L}$  solution. Higher probe concentrations would also incur a higher cost in manufacturing of the biosensor. The fraction of covalent probe immobilization was higher than 90 % of the total amount of probe added (Table 2). This immobilization efficiency is much higher than that of previously reported covalent oligonucleotide immobilization methods [47, 48]. Despite the achievement of these high immobilization efficiencies, the total amount of probe molecules that can bind to tosylated cellulose remains low because of the observed low degree of substitution to a maximum of 10 % of the available hydroxyl groups.

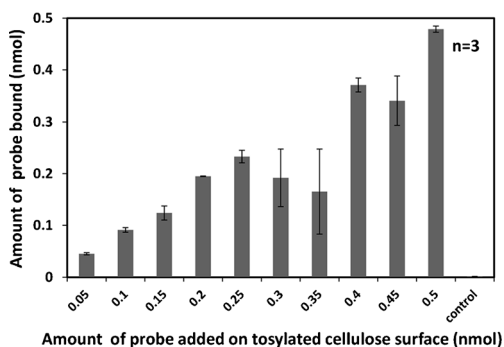


**Fig. 3** Immobilization quantities of fluorescein-labelled oligonucleotide probes on tosylated cellulose derived from the area under the curve of fluorescence intensity measurements

## DNA detection

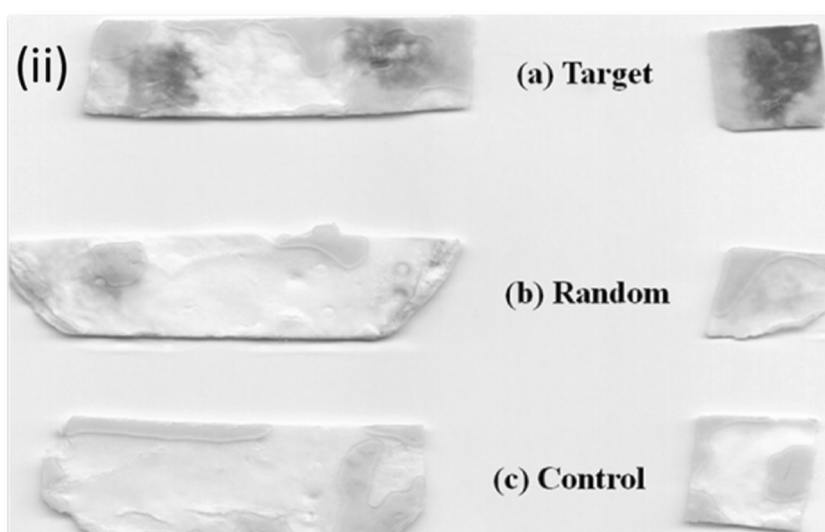
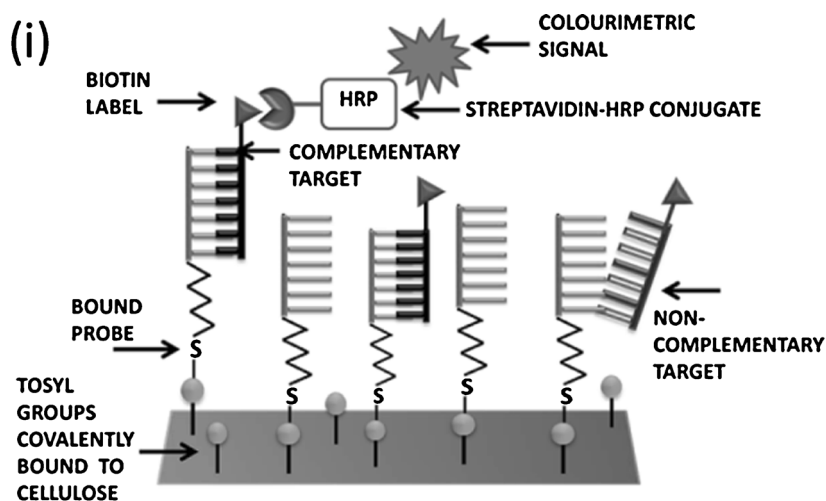
The principle of the bioassay used for DNA detection exploiting the specific hybridization of a biotin-labelled oligonucleotide with a cellulose-attached oligonucleotide probe is shown schematically in Fig. 4. The streptavidin–HRP conjugate functions as a transducer that provides a visual readout of hybridization as the biorecognition event. As the signal processing element—the human eye or a scanner—is not an integral part of the system, it must be termed a ‘bioassay’ instead of a ‘biosensor’. The results in Fig. 4 show the successful detection of target DNA complementary to the probe. Intense blue spots characteristic of 3,5,3',5'-tetramethylbenzidine oxidation via HRP/H<sub>2</sub>O<sub>2</sub> were obtained with target DNA, whereas a DNA oligonucleotide with a randomized sequence showed blue spots of lower intensity, and no blue spots were obtained in a negative control experiment without DNA oligonucleotide. The results show clearly that specific hybridization of target–probe sequences was achieved and provide indirect confirmation of successful tosylation and probe immobilization.

Covalent immobilization of oligonucleotides has been successfully used for electrochemical, optical and colorimetric DNA biosensor assays. Some of these include polypyrrole–poly(vinyl sulfonate)-coated platinum electrodes covalently linked with 25-bp polydeoxycytidine using avidin–biotin

**Table 2** Efficiency of oligonucleotide probe immobilization on tosylated cellulose

Amount of probe added (nmol)	Amount of probe immobilized covalently (nmol)	Immobilization (%)
0.05	0.045	90.08
0.10	0.091	91.098
0.15	0.124	82.59
0.20	0.195	97.44
0.25	0.232	93.16
0.30	0.192	63.95
0.35	0.165	47.21
0.40	0.370	92.70
0.45	0.340	75.73
0.50	0.478	95.76

**Fig. 4** *Top*: Schematic representation of the bioassay method. *Bottom*: Colour development on thiol-probe-immobilized tosylated cellulose strips after hybridization with complementary (target) DNA (a), non-complementary (random) DNA (b) and the control (c). *HRP* horseradish peroxidase



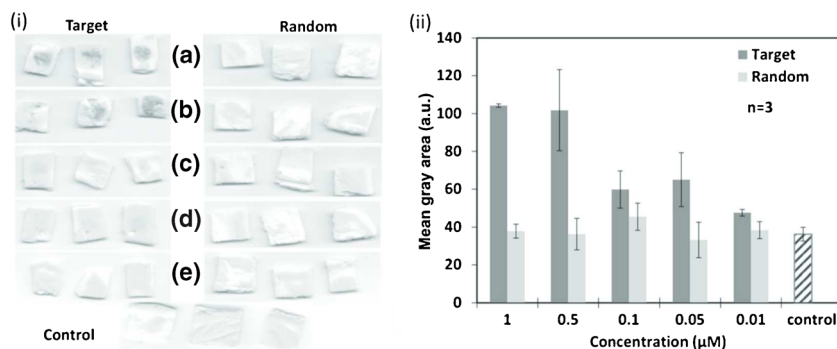
binding and carbodiimide coupling [49], amide formation using amine-functionalized probes and oxidized cellulose [7], thiol- or amine-modified oligonucleotides attached to a photoactive polystyrene surface [23] and thiol-functionalized oligonucleotides covalently linked to gold nanoparticles [50]. In the present work, the specific detection of DNA using tosylated-cellulose-linked oligonucleotide probes was demonstrated for the first time. The paper strip has the potential to be developed into an array-type sensor by chemical immobilization of oligonucleotides of different sequences at various spots, thus allowing multiplexed detection of specific various characteristics of pathogens. Within the current set-up, the spots are of irregular size, which could be circumvented by micropatterning the paper using wax printing [51].

#### Limit of detection

The detection limit of the cellulose-strip biosensor was determined by using a range of oligonucleotide concentrations

from 0.01 to 1.0  $\mu\text{M}$  (see Fig. 5 for examples). The quantitative analysis shown in Fig. 5 reveals a clear difference between target and random oligonucleotide samples up to a concentration of 0.05  $\mu\text{M}$ , which corresponds to a total amount of 5 pmol in a volume of 100  $\mu\text{L}$ . This detection limit is higher, but within a similar range of other similar DNA hybridization-based biosensors developed using oligonucleotides immobilized onto polystyrene plates or streptavidin-coated microtitre plates. These two systems also exploit  $\text{H}_2\text{O}_2$  oxidation with streptavidin-HP conjugate systems and have limits of detection of 4 nM and within the micromolar range, respectively [23, 52]. The assay sensitivity is significantly less than that of gold-nanoparticle-based DNA biosensors, which have detection limits of 200 pM and 1.1 fM [14, 24]. However, this study is a promising proof of concept for the method, and improved sensitivities may be achieved by the exploring the following avenues in further studies to increase the efficiency of the biosensor developed: increasing the tosyl chloride concentration to enhance tosylation and

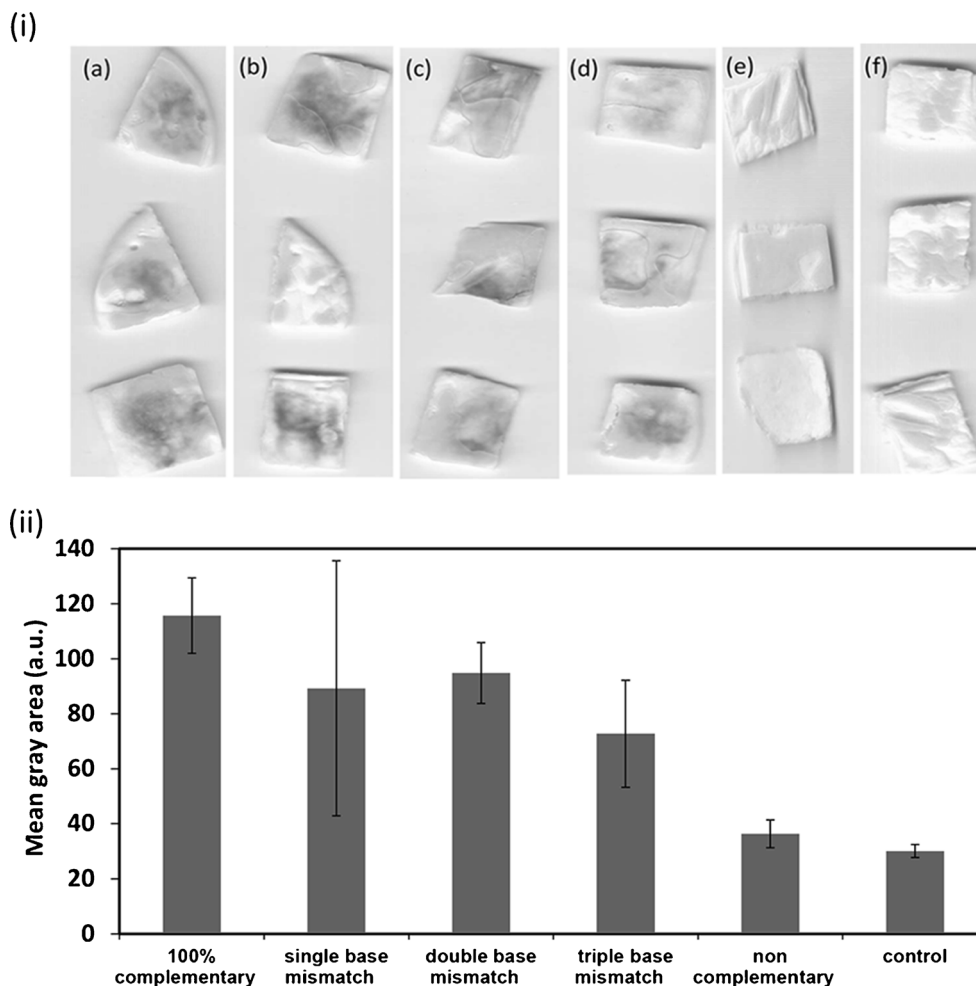
**Fig. 5** *Left:* Sensitivity analysis of the assay with target and random sequences at concentrations of 1  $\mu\text{M}$  (a), 0.5  $\mu\text{M}$  (b), 0.1  $\mu\text{M}$  (c), 0.05  $\mu\text{M}$  (d) and 0.001  $\mu\text{M}$  (e) and the control (f). *Right:* Mean grey area pixel intensity of scanned images analysed with ImageJ



subsequently increase sensitivity; using probes with higher melting points in the same gene; and investigating the use of various visual signal enhancers. Electrochemical methods based on voltammetry and impedimetry are able to achieve high sensitivity in the picomolar and femtomolar ranges [49, 53–55]; however, these methods require expensive electrodes, coating of glass electrodes and carbon nanotubes for immobilization and hybridization [56]. Optical methods using Förster

resonance energy transfer based on quantum dots and surface-enhanced Raman scattering for DNA detection have also demonstrated sensitivities of below 10 nM and 2.5 pM, respectively, but require high-cost fluorimeters and spectrometers for analysis, but these are not portable and are cumbersome to use [57, 58]. The use of cost-effective modified cellulose strips with visual detection up to 0.1  $\mu\text{M}$  could be advantageous over other methods once they have been further

**Fig. 6** *Top:* Specificity analysis of the assay with 100 % complementary target (a), single base mismatch (b), double base mismatch (c), triple base mismatch (d), non-complementary (randomized) probe (e) and negative control (f) without addition of oligonucleotides. *Bottom:* Assay specificity quantification with the mean grey area analysis of pixel intensity of scanned samples





optimized. It is possible that the sensitivity can be improved, for example, by enhancing the degree of tosylation of cellulose.

### Specificity

The specificity test was conducted to ascertain what level of base-pair mismatches could be tolerated. The biosensor was treated with oligonucleotide solution at 1  $\mu\text{M}$ , and the oligonucleotide had zero, one, two or three base-pair mismatches to the surface-attached probe (Fig. 6). The averages of the signal intensity over various experiments are shown in Fig. 6 and are compared with the negative control randomized oligonucleotide sequence. The results show an increase in signal fluctuation with base-pair mismatches, and there is an overall tendency for lower signal intensities with an increasing number of base mismatches. However, even at three base mismatches, the signal is above the level obtained for the negative control. This shows, on the one hand, that the biosensor is able to detect oligonucleotides of similar but variable sequences, but, on the other hand, the specificity is not very high. In a similar method based on DNA oligonucleotides attached to a polystyrene surface and HRP detection, up to two base-pair mismatches between a biotinylated probe and the target led to a detectable signal, whereas three base-pair mismatches were undistinguishable from a random target [23]. Most likely the specificity depends on the combination of probe and target sequences (in particular the GC content) and could be increased by choosing different probes, raising the hybridization temperature or by adding a denaturant such as formaldehyde or dimethyl sulfoxide. The melting temperature of the probe–target pair used in the current study was 68  $^{\circ}\text{C}$ .

### Hybridization time

From a practical point of view, the time required for the assay should be as short as possible. Towards that goal, the dependence of the signal intensity on the hybridization time was

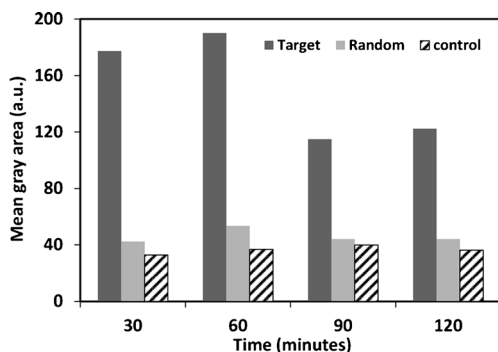


**Fig. 7** Hybridization time analysis for the assay using the mean grey area of scanned target (dark grey), random (light grey) and control (striped) samples for hybridization times of 30, 60, 90 and 120 min. The mean of two repeats is shown

investigated between 30 and 120 min (Fig. 7). Shorter hybridization times, between 30 and 60 min, produce the highest signal. It is possible that longer hybridization times lead to

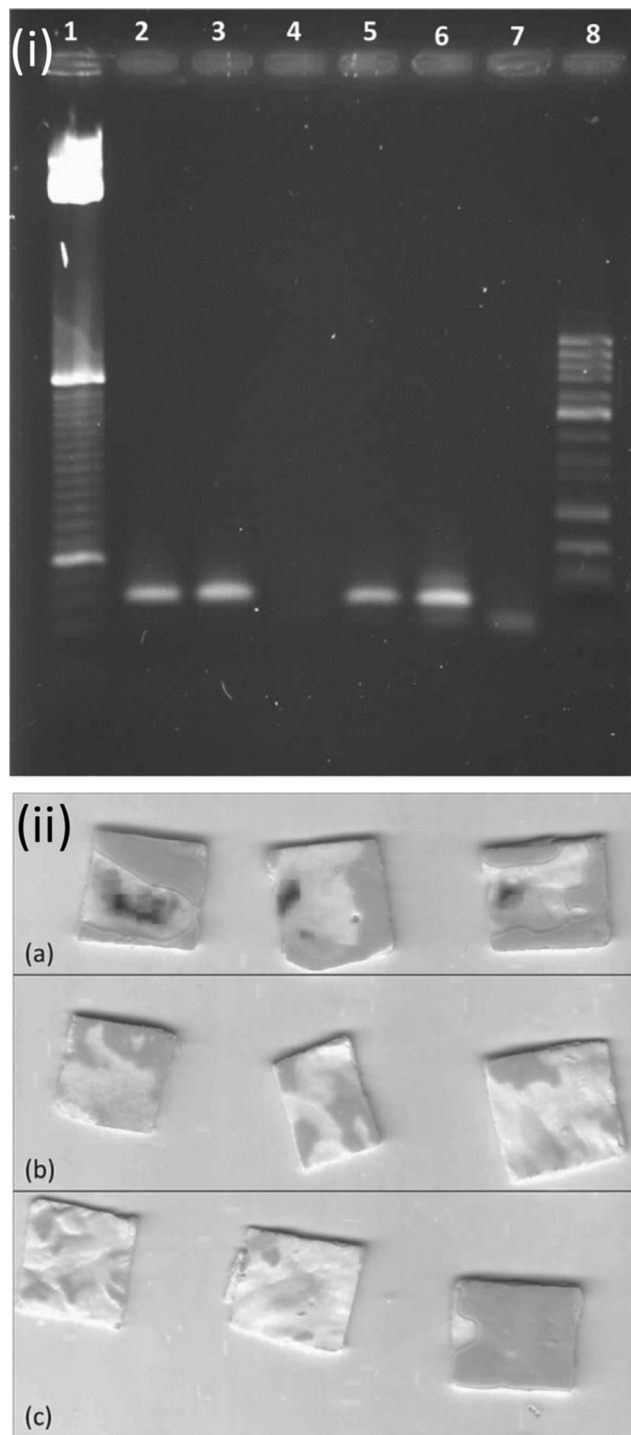


**Fig. 8** *Top*: Approximately 74-bp PCR products in 2 % agarose gel: 1 25-bp ladder; 2 and 3 bands from a PCR product complementary to the probe, 5 and 6 bands from a non-complementary PCR product, 4 and 7 controls without template DNA, 8 50-bp ladder. *Bottom*: Assay (colour development) performed with PCR products corresponding to a region complementary to the probe (a), a non-complementary region (b) and a negative control (without DNA) (c)

irreversible non-specific attachment that cannot be removed by subsequent washing steps. A 30-min hybridization time would be advantageous in a clinical or point-of-care setting, as results could be provided to the end user in a short time. These hybridization times are much more preferable to those reported earlier, which range from 5 h in a colorimetric detection method [59] to 18 h in electrochemical methods [60]. Some gold-nanoparticle-based assays can yield results in minutes; however, the colour changes in such cases are likely to be highly unstable, making them less reliable [14].

#### PCR assay

To test the cellulose-based biosensor with pathogen DNA, DNA from *M. tuberculosis* was amplified by PCR. A short region from the transposable element IS6110 was chosen, because it is a multiple copy element which is spread over the entire genome, and the location of IS6110 can be used for the identification of a particular strain. IS6110-based PCR is viable for routine use in clinical laboratories for *M. tuberculosis* in sputum samples [61]. The PCR was designed to amplify a small 74-bp sequence including the sequence complementary to the immobilized probe. A 71-bp sequence non-complementary to the probe was amplified as well and was used as the negative control. The PCR products had the expected size as shown by agarose gel electrophoresis (Fig. 8). Bands were obtained for both complementary and non-complementary products at a migration distance corresponding to 74 bp and 71 bp. The PCR products were used directly for detection without purification after denaturing at 95 °C for 10 min and rapid cooling in ice.

The results of the bioassay in Fig. 8 show that the PCR products corresponding to the complementary region of the probe yielded the expected blue colour, and the non-complementary PCR products and controls did not yield any colour, indicating that the assay was successful for the samples obtained from bacterial DNA isolates. Although the PCR is required to introduce biotin labels, even in combination with PCR the reported method has two advantages. Firstly, the method has the potential to produce array-type assays or biosensors on a cellulose surface with multiple probes that may be used to distinguish between various pathogens in one step or to determine the specific genomic type of the pathogen. Secondly, that it has the potential to provide same-day results in the field using portable PCR systems (reviewed in [62]).

In summary, we have demonstrated the successful use of tosylated cellulose strips for the chemical immobilization of oligonucleotides, and the development of a colorimetric assay for pathogenic DNA. The method has a number of advantages. It is highly cost-effective as the tosylated cellulose strips themselves could be produced easily on a large scale possibly during the process of paper manufacturing. Multiplexed detection systems could be produced by attaching

oligonucleotide probes to different spots on the surface of micropatterned paper [51]. Once the biosensor has been produced, the detection method eliminates the requirement of sophisticated instruments, except a portable PCR instrument, and the strips can be disposed of after use. The reagents and probes are used in low concentrations and can be used for many assays, hence avoiding recurring expenditure.

**Acknowledgments** This project was partially funded by the School of Life and Medical Sciences, University of Hertfordshire, UK. We thank the Veterinary Laboratories Agency, Addlestone, for providing a sample of *M. tuberculosis* DNA.

#### References

1. Song S, Xu H, Fan C (2006) Potential diagnostic applications of biosensors: current and future directions. *Int J Nanomed* 1(4):433–440
2. Albayrak N, Yang S-T (2002) Immobilization of *Aspergillus oryzae*  $\beta$ -galactosidase on tosylated cotton cloth. *Enzym Microb Technol* 31:371–383
3. Yin L-T, Lin Y-T, Leu Y-C, Hu C-Y (2010) Enzyme immobilization on nitrocellulose film for pH-EGFET type biosensors. *Sens Actuators B* 148(1):207–213. doi:10.1016/j.snb.2010.04.042
4. Schmidt EK, Liebermann T, Kreiter M, Jonczyk A, Naumann R, Offenhäusser A, Neumann E, Kukul A, Maelicke A, Knoll W (1998) Incorporation of the acetylcholine receptor dimer from *Torpedo californica* in a peptide supported lipid membrane investigated by surface plasmon and fluorescence spectroscopy. *Biosens Bioelectron* 13(6):585–591
5. Arya SK, Chomokur G, Venugopal M, Bhansali S (2010) Antibody functionalized interdigitated micro-electrode (IDmicroE) based impedimetric cortisol biosensor. *Analyst* 135(8):1941–1946. doi:10.1039/c0an00242a
6. Corso CD, Dickherber A, Hunt WD (2008) An investigation of antibody immobilization methods employing organosilanes on planar ZnO surfaces for biosensor applications. *Biosens Bioelectron* 24(4):811–817. doi:10.1016/j.bios.2008.07.011
7. Su S, Nutiu R, Filipe CDM, Li Y, Pelton R (2007) Adsorption and covalent coupling of ATP-binding DNA aptamers onto cellulose. *Langmuir* 23(3):1300–1302. doi:10.1021/la060961c
8. Ali MM, Aguirre SD, Xu Y, Filipe CDM, Pelton R, Li Y (2009) Detection of DNA using bioactive paper strips. *Chem Commun* 6640–6642
9. Stender H, Broomer A, Oliveira K, Perry-O'Keefe H, Hyldig-Nielsen JJ, Sage A, Young B, Coull J (2000) Rapid detection, identification, and enumeration of *Pseudomonas aeruginosa* in bottled water using peptide nucleic acid probes. *J Microbiol Methods* 42(3):245–253
10. Liang R-Q, Li W, Li Y, C-y T, Li J-X, Jin Y-X, Ruan K-C (2005) An oligonucleotide microarray for microRNA expression analysis based on labeling RNA with quantum dot and nanogold probe. *Nucleic Acids Res* 33(2):e17. doi:10.1093/nar/gni019
11. Liu A, Wang K, Weng S, Lei Y, Lin L, Chen W, Lin X, Chen Y (2012) Development of electrochemical DNA biosensors. *Trends Anal Chem* 37:101–111. doi:10.1016/j.trac.2012.03.008
12. Grant S, Davis F, Pritchard J, Ka L, Higson SPJ, Gibson TD (2003) Labelless and reversible immunosensor assay based upon an electrochemical current-transient protocol. *Anal Chim Acta* 495(1–2):21–32. doi:10.1016/j.aca.2003.08.026

13. Kukol A, Li P, Estrela P, Ko-Ferrigno P, Migliorato P (2008) Label-free electrical detection of DNA hybridization for the example of influenza virus gene sequences. *Anal Biochem* 374(1):143–153. doi:10.1016/j.ab.2007.10.035
14. Qi Y, Li B, Zhang Z (2009) Label-free and homogeneous DNA hybridization detection using gold nanoparticles-based chemiluminescence system. *Biosens Bioelectron* 24(12):3581–3586. doi:10.1016/j.bios.2009.05.021
15. Dolatabadi JEN, Mashinchian O, Ayoubi B, Jamali AA, Mobed A, Losic D, Omid Y, de la Guardia M (2011) Optical and electrochemical DNA nanobiosensors. *Trends Anal Chem* 30(3):459–472. doi:10.1016/j.trac.2010.11.010
16. Lazerges M, Bedioui F (2013) Analysis of the evolution of the detection limits of electrochemical DNA biosensors. *Anal Bioanal Chem* 405(11):3705–3714. doi:10.1007/s00216-012-6672-5
17. Mir M, Homs A, Samitier J (2009) Integrated electrochemical DNA biosensors for lab-on-a-chip devices. *Electrophoresis* 30(19):3386–3397. doi:10.1002/elps.200900319
18. Luo C, Tang H, Cheng W, Yan L, Zhang D, Ju H, Ding S (2013) A sensitive electrochemical DNA biosensor for specific detection of Enterobacteriaceae bacteria by Exonuclease III-assisted signal amplification. *Biosens Bioelectron* 48:132–137. doi:10.1016/j.bios.2013.03.084
19. Sahoo P, Suresh S, Dhara S, Saini G, Rangarajan S, Tyagia K (2013) Direct label free ultrasensitive impedimetric DNA biosensor using dendrimer functionalized GaN nanowires. *Biosens Bioelectron* 44:164–170. doi:10.1016/j.bios.2013.01.023
20. Kim YJ, Jones JE, Li H, Yampara-Iquise H, Zheng G, Carson CA, Cooperstock M, Sherman M, Yu Q (2013) Three-dimensional (3-D) microfluidic-channel-based DNA biosensor for ultra-sensitive electrochemical detection. *J Electroanal Chem* 702:72–78. doi:10.1016/j.jelechem.2013.04.021
21. Sassolas A, Leca-Bouvier BD, Blum LJ (2008) DNA biosensors and microarrays. *Chem Rev* 108(1):109–139. doi:10.1021/cr0684467
22. Martinez AW, Phillips ST, Carrilho E, Thomas SW III, Sindi H, Whitesides GM (2008) Simple telemedicine for developing regions: camera phones and paper-based microfluidic devices for real-time, off-site diagnosis. *Anal Biochem* 80(10):3699–3707
23. Kannoujia DK, Nahar P (2010) Single-step covalent immobilization of oligonucleotides onto solid surface. *Anal Methods* 2:212–216. doi:10.1039/c001661f
24. Reynolds RA III, Mirkin CA, Letsinger RL (2000) A gold nanoparticle / latex microsphere-based colorimetric oligonucleotide detection method. *Pure Appl Chem* 7(1–2):229–235
25. Vaseghi A, Safaie N, Bakhshinejad B, Mohsenifar A, Sadeghizadeh M (2013) Detection of *Pseudomonas syringae* pathovars by thiol-linked DNA–gold nanoparticle probes. *Sens Actuators B* 181:644–651. doi:10.1016/j.snb.2013.02.018
26. Wu Z, Wu Z-K, Tang H, Tang L-J, Jiang J-H (2013) Activity-based DNA-gold nanoparticle probe as colorimetric biosensor for DNA methyltransferase/glycosylase assay. *Anal Chem* 85(9):4376–4383. doi:10.1021/ac303575f
27. Joos B, Kuster H, Cone R (1997) Covalent attachment of hybridizable oligonucleotides to glass supports. *Anal Biochem* 24(1):96–101. doi:10.1006/abio.1997.2017
28. Bora U, Chugh L, Nahar P (2002) Covalent immobilization of proteins onto photoactivated polystyrene microtiter plates for enzyme-linked immunosorbent assay procedures. *J Immunol Methods* 268(2):171–177
29. Song F, Zhou F, Wang J, Tao N, Lin J, Vellanoweth RL, Morquecho Y, Wheeler-Laidman J (2002) Detection of oligonucleotide hybridization at femtomolar level and sequence-specific gene analysis of the *Arabidopsis thaliana* leaf extract with an ultrasensitive surface plasmon resonance spectrometer. *Nucleic Acids Res* 30(14):e72
30. Zhao W, Ali MM, Aguirre SD, Brook MA, Li Y (2008) Paper-based bioassays using gold nanoparticle colorimetric probes. *Anal Chem* 80:8431–8437
31. Bora U, Kannan K, Nahar P (2005) A simple method for functionalization of cellulose membrane for covalent immobilization of biomolecules. *J Membr Sci* 250(1–2):215–222. doi:10.1016/j.memsci.2004.10.028
32. Martinez AW, Phillips ST, Butte MJ, Whitesides GM (2007) Patterned paper as a platform for inexpensive, low-volume, portable bioassays. *Angew Chem Int Ed* 46:1318–1320. doi:10.1002/anie.200603817
33. Pelton R (2009) Bioactive paper provides a low-cost platform for diagnostics. *Trends Anal Chem* 28:925–942. doi:10.1016/j.trac.2009.05.005
34. C-m C, Mazzeo AD, Gong J, Martinez AW, Phillips ST, Jain N, Whitesides GM (2010) Millimeter-scale contact printing of aqueous solutions using a stamp made out of paper and tape. *Lab Chip* 10:3201–3205. doi:10.1039/c004903d
35. Martinez AW, Phillips ST, Nie Z, Cheng C-M, Carrilho E, Wiley BJ, Whitesides GM (2010) Programmable diagnostic devices made from paper and tape. *Lab Chip* 10:2499–2504
36. Ornatka M, Sharpe E, Andreescu D, Andreescu S (2011) Paper bioassay based on ceria nanoparticles as colorimetric probes. *Anal Chem* 83:4273–4280
37. Tian J, Shen W (2011) Printing enzymatic reactions. *Chem Commun* 47:1583–1585
38. Kim UJ, Kuga S, Wada M, Okano T, Kondo T (2000) Periodate oxidation of crystalline cellulose. *Biomacromolecules* 1:488–492
39. Jain RK, Lal K, Bhatnagar HL (1989) Thermal degradation of cellulose esters and their tosylated products in air. *Polym Degrad Stabil* 26(2):101–112
40. Heinze T, Rahnc K, Jaspers M, Berghmans H, Jena D (1996) p-Toluenesulfonyl esters in cellulose modifications : acylation of remaining hydroxyl groups. *Macromol Chem Phys* 197:4207–4224
41. Kong F, Hu YF (2012) Biomolecule immobilization techniques for bioactive paper fabrication. *Anal Bioanal Chem* 403:7–13. doi:10.1007/s00216-012-5821-1
42. Ivnitski D, Abdel-Hamid I, Atanasov P, Wilkins E (1999) Biosensors for detection of pathogenic bacteria. *Biosens Bioelectron* 14(7):599–624. doi:10.1016/s0956-5663(99)00039-1
43. Kapperud G, Vardund T, Skjerve E, Hornes E, Michaelsen TE (1993) Detection of pathogenic *Yersinia enterocolitica* in foods and water by immunomagnetic separation, nested polymerase chain reactions, and colorimetric detection of amplified DNA. *Appl Environ Microbiol* 59(9):2938–2944
44. Pires ACDS, Soares NDFF, da Silva LHM, da Silva MDCH, De Almeida MV, Le Hyaric M, Andrade NJD, Soares RF, Mageste AB, Reis SG (2011) A colorimetric biosensor for the detection of foodborne bacteria. *Sens Actuators B* 153(1):17–23. doi:10.1016/j.snb.2010.09.069
45. Rahn K, Diamantoglou M, Klemm D, Berghmans H, Heinze T (1996) Homogeneous synthesis of cellulose p-toluenesulfonates in N, N-dimethylacetamide/LiCl solvent system. *Angew Makromol Chem* 238:143–163
46. Schneider CA, Rasband WS, Eliceiri KW (2012) NIH Image to ImageJ: 25 years of image analysis. *Nat Methods* 9(7):671–675. doi:10.1038/Nmeth.2089
47. Defrancq E, Hoang A, Vinet F, Dumy P (2003) Oxime bond formation for the covalent attachment of oligonucleotides on glass support. *Bioorg Med Chem Lett* 13:2683–2686
48. Okutucu B, Telefoncu A (2004) Covalent attachment of oligonucleotides to cellulose acetate membranes. *Artif Cells Blood Substit Immobil Biotechnol* 32:599–608
49. Arora K, Prabhakar N, Chand S, Malhotra BD (2007) Immobilization of single stranded DNA probe onto polypyrrole-polyvinyl sulfonate

- for application to DNA hybridization biosensor. *Sens Actuators B* 126(2):655–663. doi:10.1016/j.snb.2007.04.029
50. Storhoff JJ, Elghanian R, Mucic RC, Mirkin CA, Letsinger RL (1998) One-pot colorimetric differentiation of polynucleotides with single base imperfections using gold nanoparticle probes. *J Am Chem Soc* 7863(97):1959–1964
51. Carrilho E, Martinez AW, Whitesides GM (2009) Understanding wax printing: a simple micropatterning process for paper-based microfluidics. *Anal Chem* 81(16):7091–7095. doi:10.1021/Ac901071p
52. Mir M, Lozano-Sánchez P, Katakis I (2008) Towards a target label-free suboptimum oligonucleotide displacement-based detection system. *Anal Bioanal Chem* 391:2145–2152. doi:10.1007/s00216-008-2119-4
53. Chen C-P, Ganguly A, Lu C-Y, Chen T-Y, Kuo C-C, Chen R-S, Tu W-H, Fischer WB, Chen K-H, Chen L-C (2011) Ultrasensitive in situ label-free DNA detection using a GaN nanowire-based extended-gate field-effect-transistor sensor. *Anal Chem* 83(6):1938–1943. doi:10.1021/ac102489y
54. dos Santos Riccardi C, Kranz C, Kowalik J, Yamanaka H, Mizaikoff B, Josowicz M (2008) Label-free DNA detection of hepatitis C virus based on modified conducting polypyrrole films at microelectrodes and atomic force microscopy tip-integrated electrodes. *Anal Chem* 80(1):237–245. doi:10.1021/ac701613t
55. Wang J, Li S, Zhang Y (2010) A sensitive DNA biosensor fabricated from gold nanoparticles, carbon nanotubes, and zinc oxide nanowires on a glassy carbon electrode. *Electrochim Acta* 55(15):4436–4440. doi:10.1016/j.electacta.2010.02.078
56. Teles F, Fonseca L (2008) Trends in DNA biosensors. *Talanta* 77(2):606–623. doi:10.1016/j.talanta.2008.07.024
57. Kim Y, Sohn D, Tan W (2008) Molecular beacons in biomedical detection and clinical diagnosis. *Int J Clin Exp Pathol* 1(2):105–116
58. Qian X, Zhou X, Nie S (2008) Surface-enhanced Raman nanoparticle beacons based on bioconjugated gold nanocrystals and long range plasmonic coupling. *J Am Chem Soc* 130(45):14934–14935. doi:10.1021/ja8062502
59. Bai X, Shao C, Han X, Li Y, Guan Y, Deng Z (2010) Visual detection of sub-femtomole DNA by a gold nanoparticle seeded homogeneous reduction assay: toward a generalized sensitivity-enhancing strategy. *Biosens Bioelectron* 25:1984–1988. doi:10.1016/j.bios.2010.01.012
60. Tam PD, Van Hieu N, Chien ND, Le A-T, Anh Tuan M (2009) DNA sensor development based on multi-wall carbon nanotubes for label-free influenza virus (type A) detection. *J Immunol Methods* 350:118–124. doi:10.1016/j.jim.2009.08.002
61. Menéndez C, Samper S, Ota I, García MJ, Universitario H, Servet M (2012) IS6110 the double-edged passenger. In: Cardona P-J (ed) *Understanding tuberculosis - deciphering the secret life of the Bacilli*. InTech, Rijeka, pp 59–89. doi:10.5772/32046
62. Almassian DR, Cockrell LM, Nelson WM (2013) Portable nucleic acid thermocyclers. *Chem Soc Rev* 42(22):8769–8798. doi:10.1039/C3cs60144g